Bulletin of Environment, Pharmacology and Life Sciences
Bull. Env.Pharmacol. Life Sci., Vol 4 [Spl issue 1] 2015: 160-169

Online ISSN 2277-1808
Journal's URL:http://www.bepls.com
CODEN: BEPLAD
Global Impact Factor 0.533
Universal Impact Factor 0.9804

FULL LENGTH ARTICLE **OPEN ACCESS**

Study effect of base -shaped spindle, Rounded corner rectangle, square, Rectangular and oval on the lateral velocity variations, flow patterns and shear stress of the riverbed by Open FOAM

Marieh Rajaie
PhD student of Water and Hydraulic Structure Engineering, Hydraulic Structure Faculty, Department of Civil Engineering, Islamic Azad University of South Branch, Tehran, Iran
E-mail: marierajaie@yahoo.com

ABSTRACT
Today the scour issue is one of the most important issues in the river engineering science, so that the destruction of the most built up bridges in the rivers are mostly not for structural reasons but only for the hydraulic factors in the design of bridges. Base and sides of the bridge deviates the flow that the result is scour in adjacent of the structure. In this study, we compare and evaluate the longitudinal and lateral velocity variations, flow pattern and riverbed shear stress around the bridge's base with spindle-shaped sections, rounded corner rectangles, squares, rectangles and ovals. Three-dimensional modeling is done by OpenFOAM software. The flow turbulent using ε k- RNG turbulence model take into the accounts and the equations of the turbulence are Navier-Stokes (Reynolds equations). The results show that the shape of the bridge's base had great influence on the lateral velocity variations and the flow pattern that is effective in prediction of the scour and bed model. The results indicates that the rate of longitudinal, lateral velocity variations, flow separation, and also the bed shear stress, respectively, around the bases of the spindle, oval, rounded corners rectangle, square and rectangle is low that as the result the scouring around the bases occur less frequently.
Key words*: the pier, software OpenFOAM, changes transverse velocity, flow pattern, shear stress*

INTRODUCTION

Generally, scour at the bridges divide into two categories of the general scour and the local scour. If in the range of the bridge construction, the river bed washed and with regard to the natural bed of the river in upstream will be in the lower level and is called the general scour. The local scour refer to the going down of the riverbed around the built up structures in it toward the bed level ,after going down due to the general scouring. Local scour around the bridge piers is created by a vortex system. The vortex system is created by the flow diversion of the piers. The main vortex system that helps to the formation of the scour holes is created by the collision of flow to the forepart of the pier and its deviation to he down direction. The downward flow after collision to the riverbed dig a hole in front of the pier that inside the hole a rotating flow was created and gradually the hole 'depth will be increased. The rotating flow in front of the pier develops to the both sides of it and takes a form that in the plan resembles a horse shoe ;hence, it is called a horseshoe vortex. By passing from the side of pier, a series of secondary flows occur that these secondary flows are the main factors of the local scour occurrence. Richardson et al. (2001) showed that the local scour is the main reason of the bridge's pier destruction. The secondary flows consist of the wake vortex, trailing vortex, horseshoe vortex and bow wave system (Figure 1) [2].

According to the research conducted by Yanmaz (2001), modeling of the scouring mechanism is very complex and a unique approach to the general conditions of the river flow, sediment and characteristics of the bridge pier has not been considered. The most important factor of the scour's hole creation at front of the piers is the horseshoe vortex. At the time of the water flow clashes with the cape of the bridges' pier will convert to a pressure on the pier. Since the velocity will be decreased from the surface to the bottom, the dynamic pressure on the cape will be decreased from up to down and the created pressure gradient led to a downward flow. This downward flow after clash with the riverbed digs it and scatter in different directions (Figure 1). Homayoon and Keshavarzi in 2007 had studies on the effect of the radial waterborne installation distance on the volume and depth of the scour in downstream of the bridge pier with a circular

section [3]. According to the carried out research in New Zealand, at least one of the major occurred scours in the year can be attributed to the bridge pier scour [7].

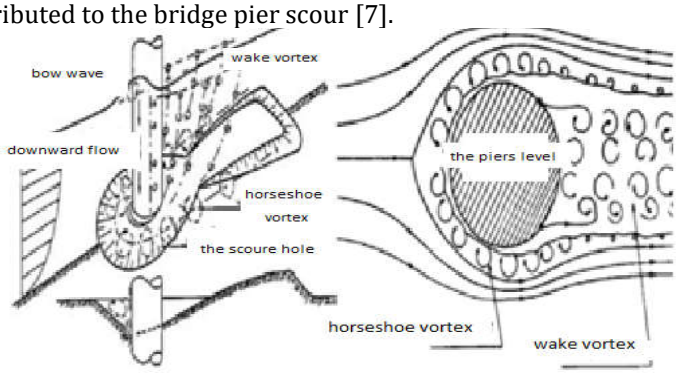

Fig (1) Display horseshoe vortex formation and uplift

SOFTWARE INTRODUCTION

OpenFOAM is an abbreviation for Field Operation and Manipulation open source. This is a functional software to numerical simulation of flow and sediment in the river and hydraulic engineering. One of the advantages of this software is provide new tools and solutions based on the problem related knowledge. Therefore, the user can identify unknowns, physical parameters and other basic variables of the problem and on the other hand with programming techniques create a file. The most important capability of the OpenFOAM software in compare with other models of CFD is the manipulation possibility of the default files and even introduction of the unknown relations with the software.

The governing equations for the turbulent flows

The governing equations of an incompressible fluid motion in the turbulent state by the Navier-Stokes equations are averaged and by the so-called Reynolds (RANS) are expressed. Simplification of the differential equations in this software was done by the finite volume method and their discretization by the central difference method.

$(RNG)k-^{\varepsilon}$Turbulence model

in$(RNG)k-^{\varepsilon}$turbulence model, the related equations of K kinetic energy and its decay rate(ε) follows [4]:

$$\rho\frac{Dk}{Dt}=\frac{\partial}{\partial x_i}\left[\alpha_k u_{eff}\frac{\partial k}{\partial x_i}\right]+G_k+G_b-\rho\varepsilon-Y_M \quad (1)$$

$$\rho\frac{D\varepsilon}{Dt}=\frac{\partial}{\partial x_i}\left[\alpha_k u_{eff}\frac{\partial \varepsilon}{\partial x_i}\right]+G_{1\varepsilon}\frac{\varepsilon}{K}(G_k+G_{2\varepsilon}G_b)-G_{1\varepsilon}\rho\frac{\varepsilon^2}{K}-R \quad (2)$$

Wherein,$G_b$is the turbulence generation due to the floating and $Y_m$is the incompressibility reagent. Also, $G_k$define as:

$$G_k=\overline{\rho u_i' u_j'}\frac{\partial \mathrm{u_j}}{\partial \mathrm{x_i}} \quad (3)$$

Constants of the model are$G_{2\varepsilon}=1.68$ and $G_{1\varepsilon}=1.68$. In this model,the viscosity turbulence is obtained from the (8) differential equation:

$$d\left(\frac{\rho^2 k}{\sqrt{\varepsilon\mu}}\right)=1.72\frac{\hat{\nu}}{\sqrt{\hat{\nu}^3-1+C_\nu}}d\hat{\nu} \quad (4)$$

Wherein,$\hat{\nu}=\frac{\mathrm{u_{eff}}}{\mu}$and $C_\nu\approx 100$. In the above Reynolds numbers, the viscosity turbulence is written similar to the standard model:

$$\mu_t=-\rho C_\mu\frac{\varepsilon^2}{K} \quad (5)$$

Wherein,C_μ coefficient is equal to 0.0845

The sensitivity survey of the model

In each model, it is necessary to be sure from the accuracy of the obtained results before the software output and analyze sits results. So that, the flow analyze first was done on the simple and specific states and then compared with the results of other researchers to ensure from the accuracy of the results. In this study, in order to ensure from accuracy of the affecting parameters on the phenomenon (mesh, suitable turbulence and flow model), the conducted experiment of Dargahi in 1989 is used [8]. As , you can see in table (1),in meshing with 122400 networks, the coefficient of determination $R\hat{}2$ is near to 1 number, the necessary time for application of the model is less and values of RMSE (mean of the relative error absolute limit) is less than other meshes , so it is selected as the optimal mesh.

Table (1) Selection of appropriate mesh

Z						X						
(nets 122400)		(nets 183600)		(nets 244800)		(nets 244800)		(nets 298800)		(352800 nets)		distance
RMSE		RMSE		RMSE		RMSE		RMSE		RMSE		x/D
0.243	0.886	0.231	0.887	0.189	0.889	0.189	0.889	0.178	0.893	0.169	0.895	-0.73
0.213	0.986	0.203	0.988	0.195	0.989	0.195	0.989	0.187	0.99	0.178	0.991	8
4hours		10 hours		17 hours		17 hours		2 hours		29 hours		time

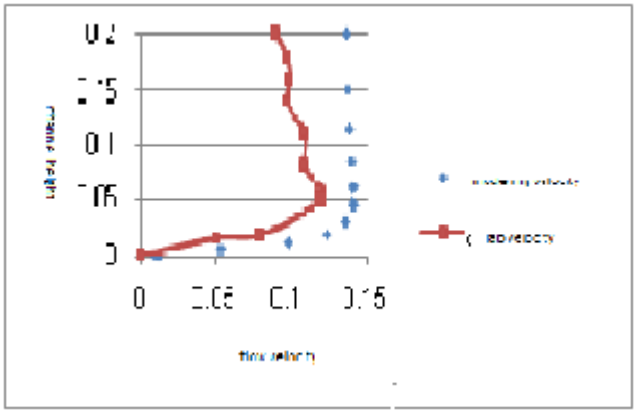

Chart (1) laboratory velocity chart and the modeled sample velocity based on the height with the input velocity of U = 0.26 in $\frac{X}{D} = -0.73$ distance from the bridge pier

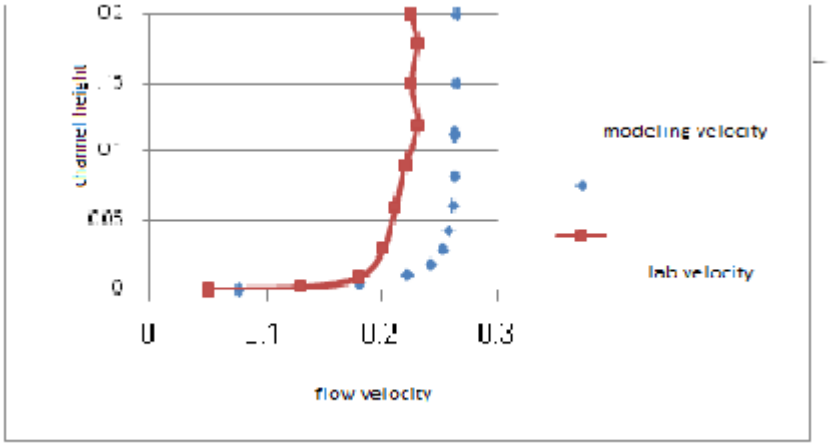

Chart (2) laboratory velocity chart and the modeled sample velocity based on the height with the input velocity of U=0.26 $\frac{m}{s}$ in $\frac{X}{D} = 8$distance from the bridge pier

Charts 1 and 2 discuss about drawing the flow velocity variations toward the depth in two distances $\frac{X}{D} = 8$and $\frac{X}{D} = -0.73$ from the pier. As mentioned intable 1, the error rate and the measured velocity difference in the laboratory and calculated by the software in $\frac{X}{D} = 8$ distance toward the pier is equal to 0/213 and in$\frac{X}{D} = -0.73$ distance toward the pier is equal to 0/243.

Turbulence realizable K-epsilon				Turbulence K-epsilon standard				Turbulence RNG K-epsilon			
RMSE	X		ratio	RMSE	X		ratio	RMSE	X		ratio
0.226	0.48	0.636	$\frac{X}{D} = -0.73$	0.211	0.535	0.852	$\frac{X}{D} = -0.73$	0.047	0.610	0.865	$\frac{X}{D} = -0.73$
0.613		0.781	$\frac{X}{D} = 8.0$	0.294		0.982	$\frac{X}{D} = 8.0$	0.190		0.989	$\frac{X}{D} = 8.0$

Table (2) the obtained result of the flow analyze by the different turbulent models

Calibration of the model toward the turbulence

Since the Reynolds number is in the $4340^{\times 10\text{^}3}$ modeling, the turbulent flow regime is intended. Therefore, to calibrate the model and select the best turbulence model, the RNG K-ε standard, K-ε standard and realizable K- ε standard were used and for each of them , the velocity near the pier from the obtained software with the flow velocity at the same place of the portal test in 1989were compared. These analyses showed that the RNG K- turbulence model is more accurate than other turbulence models. The results of this analysis are presented in Table 2. According to this table, $R\text{^}2$ determination coefficient and X coefficient of the fitting line in the RNG K-ε turbulence model than the other models is nearer to the number 1, also the value of RMSE in this state than the other turbulence models is less that indicate the more accuracy of the obtained results from the turbulence model of RNG K-ε .

Modeling

In this section, the channel modeling with the RNG K-ε turbulence model and meshing with 122,400 networks are used with different levels to study the flow pattern around the pier of the bridge and the only difference is in the base form of the pier. The channel has 20 m length and4 m width. The velocity of the flow 3.1m/s and its bed sediments have 31.4mm diameter.

Details of the modeled piers 'dimensions

In this research, we study modeling of five forms of pier with spindle, rounded corner rectangle, square, rectangle and oval forms. Dimensions of the piers are defined in accordance to the conducted researches of Hasanzadeh et al in 2011[6]. Distance of the piers from each other is determined in accordance to the conducted researches of Heidarpoor et al in 2010 [9]. Table (3) defines dimensions and distance of the piers. Based on Li and colleagues' studies in 1961, the pier form is an important factor, which has significant effect on the scour depth, because the strength of the horseshoe vortex depends on the pier form. Square, rectangle, rounded corners rectangle and oval piers respectively in contrast to the spindle pier create the maximum scour depth.

Build of bridges with the pier form which are correspond to the flow lines, reduce the flow separation and has an important effect on the scour reduction, in such a way that if the pier form was parallel with the flow lines, strength of the horseshoe vortex system strongly is reduced and less scour will be occurred[5].

Table (3) characteristics of the piers dimensions

Pier form	Small diameter(side)	Big diameter(side)	Pier form
1.68	0.42	0.84	spindle
1.68	0.42	1.26	Rounded corners rectangle

Study the flow lines around the piers

The bridge piers with reduction of the river level significantly effect on the flow pattern. The flow lines with approaching to the bridge pier change its arrangement and follow the pier geometric structure, a different pattern of the flow will be emerged. For example, Tseng et al (2000) reported that the resistance of the flow pattern in wake and horseshoe vortexes around the square piers is more than the curvature piers [10]. In fact, the bridge piers are constructed in different forms, and most of them can have the non-uniform lateral surface in height [11]. Erosion around the pier and the sedimentation rate in its downstream follow the flow patterns. The flow in the pier with the complex Horseshoe vortex system, which has begun at the upstream of the pier and the wake vortex at the downstream of the pier combined. [12] [13] [14]

As shown in Figure 2, based on the flow pattern around the pier, it is clear that the flow separation around the spindle pier was less than the other piers, therefore the less turbulence rate and ultimately the scour will be less. Images of the flow lines indicate that the generated vortexes at the downstream of the spindle pier have less strength than the other pier.

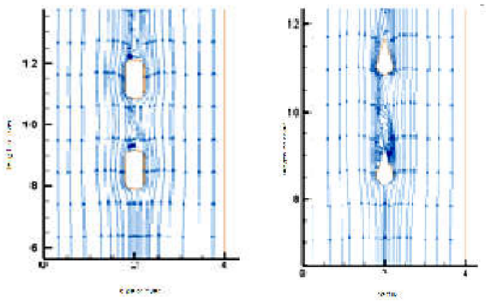

Rounded corners rectangle pier spindle pier

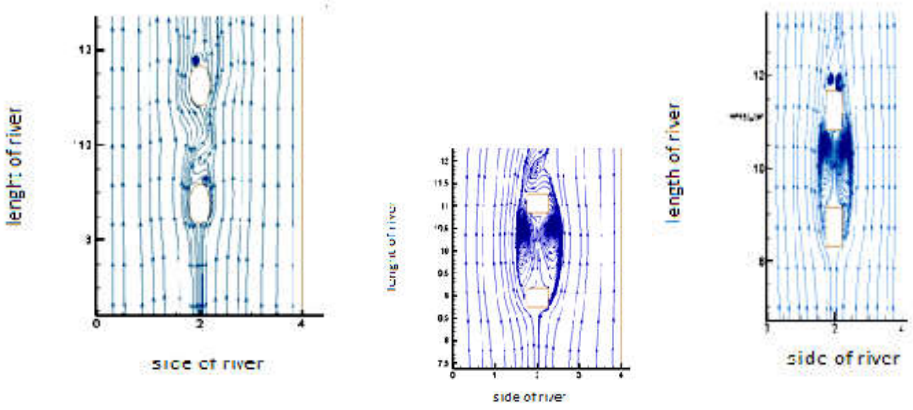

Oval pier rectangle pier square pier

Fig (2) images of the flow lines around the piers

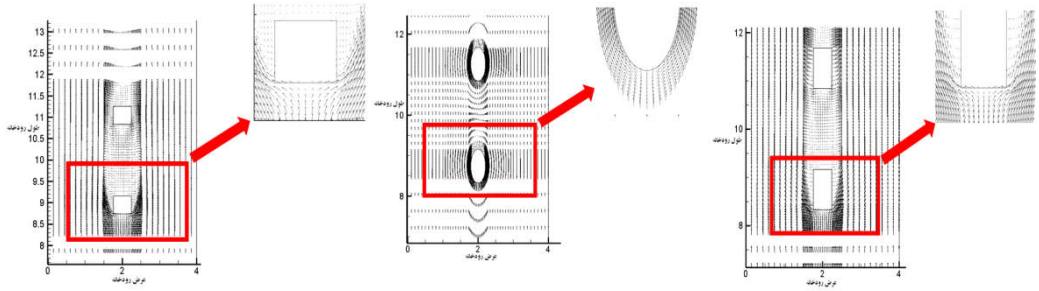

Oval pier square pier rectangle pier

Fig (3) image of the velocity vector around the piers

Evaluation of the scour threshold velocity

Now, the threshold velocity of the erosion (critical velocity (V_{cr})) is investigated. If the flow velocity in the channel is more than the velocity rate, the channel bed around the pier will be scoured and if not in the bottom of the river, the sedimentation phenomena will be occurred. The threshold velocity may be obtained from the following equation:

$$V_{cr} = \sqrt{gRS}$$

Which in this relation:

V_{cr} : critical shear velocity, g($\frac{m}{s}$): acceleration ofgravity, R($\frac{m}{s^2}$) hydraulic radius, S: the slope of the channel bed that the hydraulic radius value is obtained from the following equation:

$$R = \frac{A}{P}$$

To calculate the critical bed shear stress, the following equation is used:

$$D_{50} = 11RS \Longrightarrow D_{50} = 11\frac{\tau_{cr}}{\gamma} \Longrightarrow \tau_{cr} = \frac{\gamma . D_{50}}{11}$$

Since,D_{50} in the riverbed is equal to 31.4 mm and is more than 6 mm, indicating that the riverbed is covered with sand. On the other hand, $\tau_{cr}$is calculated from the following equation:

$$\tau_{cr} = \gamma RS \Longrightarrow \gamma RS = \frac{\gamma \times D_{50}}{11}$$

Then continue to calculateV_{cr} based on the Manning relation:

$$n = 0.048(D_{50})^{\frac{1}{6}} \Longrightarrow n = 0.027$$

$$V_{cr} = \frac{1}{n} R^{\frac{2}{3}} S^{\frac{1}{2}} \Longrightarrow V_{cr} = \frac{1}{0.027} \times 0.2196^{\frac{2}{3}} \times 0.013^{\frac{1}{2}} = 1.53 \ \frac{m}{s}$$

Since the flow velocity in the channel is3.1 $\frac{\text{m}}{\text{s}}$. This indicates that the flow velocity in the channel is greater than the critical velocity and thus the scour will occur around the pier in the channel bed.

Study of the lateral velocity variations

Charts 3 and 4 show the lateral velocity variation along the channel and at the one-meter distance from the right side of the pier for the spindle and the square piers. The lateral velocity variations in heights of 0.3, 0.48 and 0.68 m from the bed and 0.86 m away from the water surface is considered. EvaluateU_x velocity in each of the five modeled piers (charts 3 and 4) showed its increase and growth at immediately after the pier and its wings. In addition, at the back of the pier due to the presence of the wake vortexes because of its circulating nature, the increased lateral velocity components in the areas away from these vortexes are found. Comparison of the following charts can be based on the principle that the velocity variations around the spindle pier in compare to the other piers is less and the square pier due to the sudden flow separation in reaching to the pier and creation of the stronger vortexes provide the maximum velocity variations. Moreover, the lateral velocity near the pier has negative value but after pass from the pier has positive velocities. Before the flow reaches to the pier, the lateral velocity due to the velocity reduction and creation of the downward flow will find a negative value.

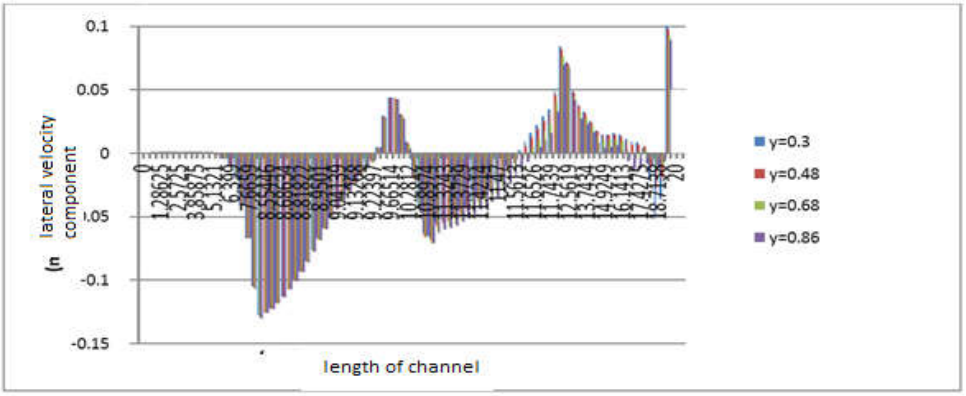

Chart (3) the component variations of the lateral velocity at 1 m distance from the right side of the spindle pier

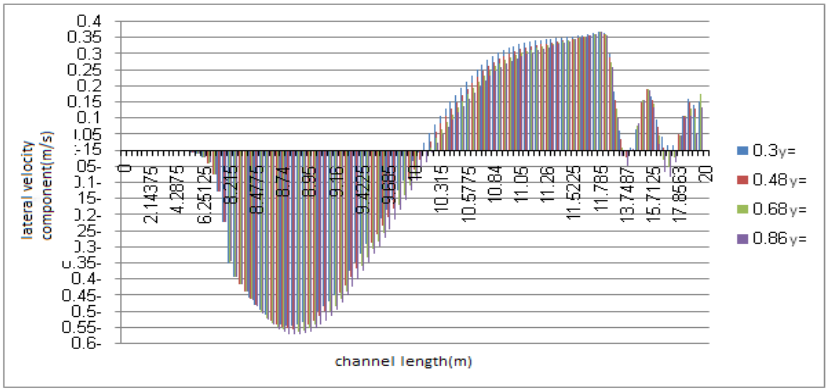

Chart (4) the component variations of the lateral velocity at 1 m distance from the right side of the square pier

In 5 and 6charts, the lateral velocity profiles for the spindle and the square piers have been studied. Due to the figures and observe of the velocity variations in the lower levels, the effect of the horseshoe vortex can

be seen in the upper parts of the pier. According to the charts, while the is reaching to the pier, due to the effects of the narrow passing way and effect of the downward flow at front of the pier , increase of the velocity will be significant. In accordance to the lateral velocity variations in height, we can see that with increase of the height, the lateral velocity variation due to the strength of the wake vortex in high heights is decreased. In chart 6, effect of the secondary flow can be seen at the front part of the pier at the second level.

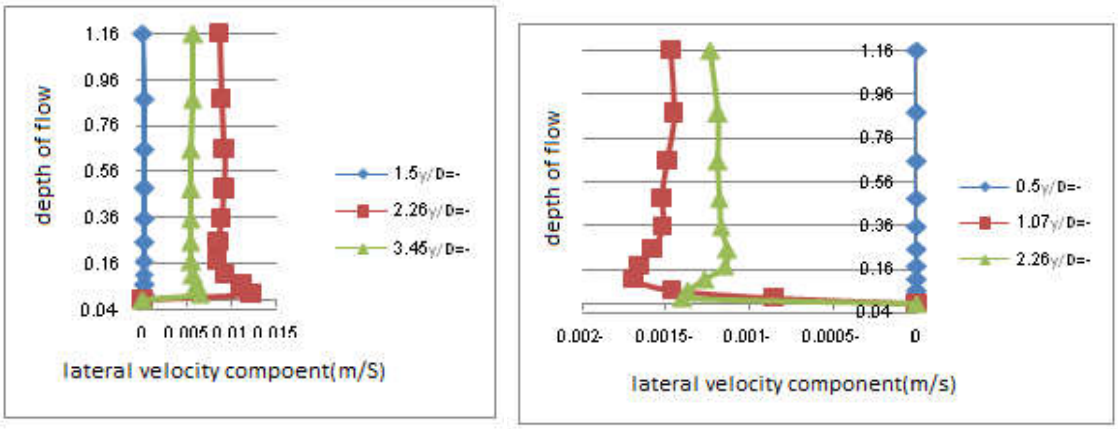

Chart (5), the deep profiles of the lateral component of the flow velocity for the upward of the bridge pier

The first row at the central axis of the Flume

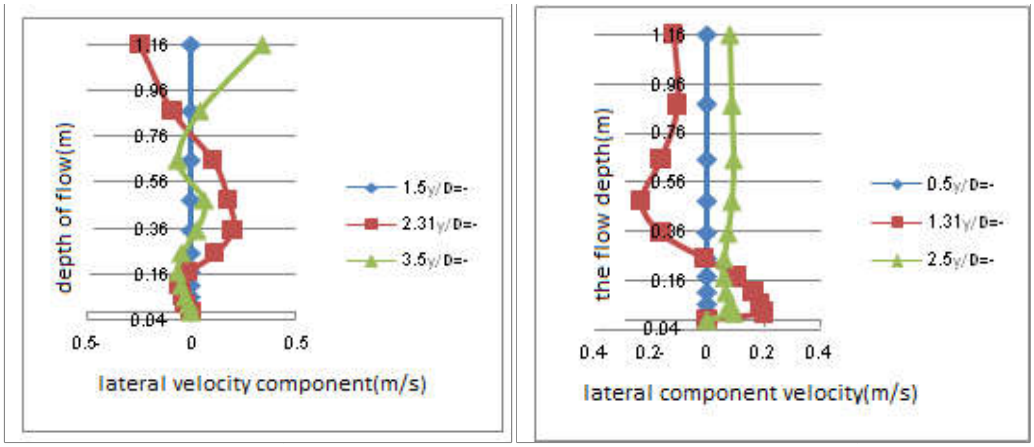

Chart (6), the deep profiles of the lateral component of the flow velocity for the upward of the bridge pier
The first row at the central axis of the Flume

Study the shear stress distribution of the bed around the pier

In the turbulent flows to calculate the exerted shear stress on the bed, we can use the turbulent stresses known as the Reynolds stresses. The calculated stress in the OpenFOAM software is based on the exerted stresses on the fluids. Due to this point, the stress of in this software can be obtained by the following equation [15]:

$$\tau = \mu \frac{\partial u}{\partial y} \qquad (6)$$

μ: Dynamic viscosity, which is equal to $10^{-5}\ \frac{\text{kg}}{\text{m.s}}$ at 20 degrees for water

$\frac{\partial u}{\partial y}$: represents the velocity variations in the flow depth

μ (Dynamicviscosity) represents the fluid properties and states the relationship between the stress and the strain. The fluid can be Newtonian and in it, the viscosity is constant or non-Newtonian which in it the

viscosity varies. In this paper, Newtonian fluid and water is considered. To compare the shear stress rate around the piers, the total normalize stress around them has been calculated. This method in fact is the study of sensitivity to the stress. This stress by the equation (5) is calculated. While the number is getting closer to the 1 number, show the more effectiveness of the shear stress on the place. In this study, the maximum normalized rate of the shear stress and their critical locations in upward of the pier at the first row between the piers and the downward of the pier at the second row are brought. Finally, the average shear stress rate at the bottom of the piers and at the critical locations has been compared with each other. If the rate of the occurred stress in the bottom is more than the calculated value at the beginning of the study ($0.028\ \frac{kn}{m^2}$) , in the context, the erosion and the bed scour will be occur that in Figure 4 are shown from the yellow to blue. In table 3, the normalized values of the shear stress at critical intervals are shown. In table 4, the average values of the shear stress are shown. In accordance to the table 4, the average values of the shear stress in bottom of the spindle pier respectively is less than the oval, rounded corners rectangle, square and rectangle piers, so the turbulence value around this pier will be occur less. In table (4), the contour image of the shear stress in the riverbed and near to the piers is seen.

$$\acute{\tau}_{total} = \frac{\tau_{total} - \tau_{total}min}{\tau_{totalmax} - \tau_{totalmin}}$$

Table (4) study the effectiveness value of the total stress on the piers

Total stress	Critical distances	Pier form
0.0135	6.19865	Rounded corners rectangles
0.0094	10.126	
0.0118	16.9988	
0.0134	3.00125	spindle
0.0031	10.84	
0.0101	16.57	
0.0137	5.81642	rectangle
0.0110	11.848	
0.0153	16.9988	
0.0147	6.19865	square
0.0127	10.6302	
0.0178	15.3302	
0.0135	6.19865	oval
0.0038	10.126	
0.0111	14.1835	

Table (3) Study the effectiveness value of the total normalized stress in the

Total normalized stress	Critical distances	Pier form
1	6.19865	Rounded corners rectangle
0.860	10.126	
0.805	16.9988	

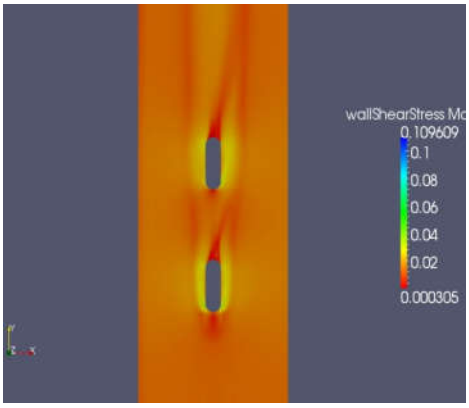

Rounded corners rectangle pier

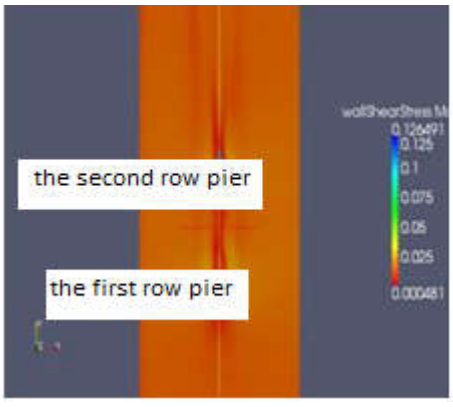

spindle pier

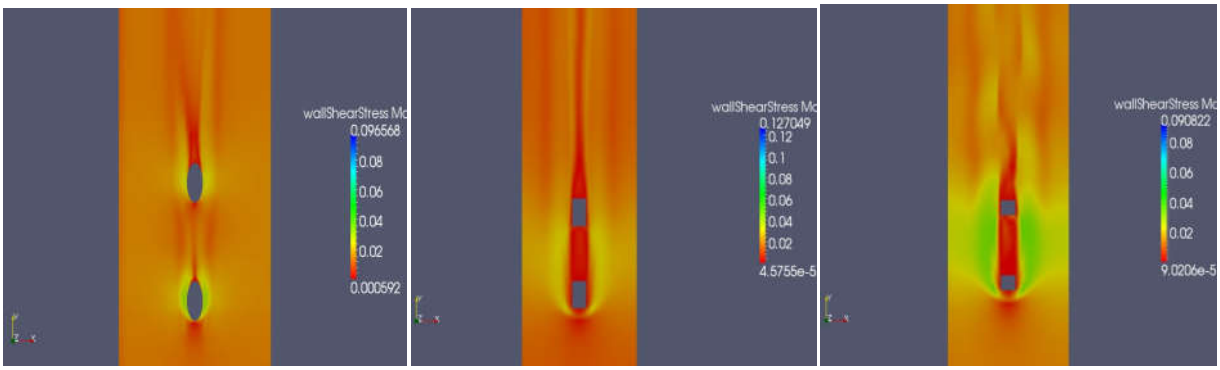

oval rectangle square pier

Figure (4) The shear stress distribution around the piers with different forms

CONCLUSION

1. Based on the verifications, the measured velocity difference rate in the lab and the measure velocity by the OpenFOAM software in distance $\frac{X}{D} = 8$ from the pier is equal to 0.213 and in distance $\frac{X}{D} = -0.73$ from the pier is 0.243.
1. Based on the turbulence model verifications, RNG K-ε has more accuracy.
2. The results of the numerical model show that the spindle pier due to the least flow separation and lower scour depth is the optimum pier form respectively in compare with the oval, rounded corners rectangle, rectangle and square piers.
3. Comparison of the lateral velocity variations' charts show that the lateral velocity variations are less around the spindle pier than the other piers.
4. In the turbulence models comparison can be seen that the power of vortices around the spindle pier is less and it is a reason for the less flow separation for this pier and least formation of the destructive emotional vortices.
5. From comparison of the maximum shear stress rates in the critical distances, the result is that the velocity variation around the spindle pier creates less shear stress and ultimately the less scour will be created around the pier.

ACKNOWLEDGMENTS

Many thanks to Dr. Reza Pirestani and Dr. S .Hassan Ghoreishi Najaf Abadi ,undoubtedly without their assistance and guidance , we aren't able to collect the paper.

REFERENCES

1. Shariati, H and Khodashenas and Ismaili (2012), evaluation of the Gap Width in reduction of local scour at the bridge pier, first research- applicable national conference of water supply, Iran.
2. Homayoon and Shokri (2011), effect of the pier form onthe depth and scour profile around the bridge pier, 11th Seminarof watering and the evaporation reduction, Kerman, Iran
3. Homayoon, Keshavarzi (2008), the effect of the installation distance of the radial waterborne on the volume and depth of the scour in downward of the bridge pier with the rounded pier. The Fourth National Congress of Civil Engineering, Tehran University, May.
4. Bushehri,Montazerian and Naderan Tahan (2011), Numerical modeling and study the combined effects of the input on the sedimentation pond efficiency with FTC drawing method using OpenFOAM software, 9th International Congress of Urbanization Engineering , Isfahan , Iran.
5. Hassounizadeh , 1991, Study experimental methods to predict the local scour around the bridge pier, Master Thesis, Shahid Chamran University, Ahvaz, Iran
6. Hassanzadeh , Hakimzadeh, Ayari .(2011). Study effects of different forms of the pier on the flow pattern around it using the Fluent software, Journal of Water Resources Research of Iran,
7. Melville, B. W., and Coleman, S. E. (2002). "Bridge scour", Water Resources Publications, LLC, Colorado, USA
8. Dargahi, B. (1989), "The turbulent flow field around a circular cylinder." Journal of Experiment in Fluids, 8, 1-12
9. Heidarpour, M. Afzalimehr, H. Izadinia, E. (2010). "Reduction of local scour around bridge pier groups using collars", International Journal of Sediment Research 25 (2010) 411-422
10. Tseng, MH, Yen, CL, Song, CS, (2000). Computation of three-dimensional flow around square and circular piers. International Journal of Numerical Methods in Fluids 34 (3), 207-227.
11. Melville, BW, Raudkivi, AJ, (1996). Effects of foundation geometry on bridge pier scour. J. Hydrol. Eng. ASCE 122 (4), 203e209.

12. Breusers H N C, Nicollet G, Shen H W. (1977). -Local Scour around cylindrical piers. Journal of Hydraulic Research, 15 (3): 211-252.
13. Melville, B.W. and Raudkivi, A.J. (1977). -Flow Characteristics in Local scour at Bridge Piers, J. Hydr. Res. IAHR, 15, 373-380.
14. Dargahi, B. (1990). -Controlling Mechanism of Local Scouring, J. Hydr. Engrg. ASCE, 116 (10), 1197-1214.
15. Payandeh. M, (2012)."Implement of a Temperature dependent Viscosity Model in OpenFOAM", a course at Chalmers University of Technology.